Ultrasound imaging of the brain using full-waveform inversion

Taskin, Ulas; Solberg Eikrem, Kjersti; Naevdal, Geir; Jakobsen, Morten; Verschuur, Dirk J.; Van Dongen, Koen W.A.

DOI
10.1109/IUS46767.2020.9251665

Publication date
2020

Document Version
Accepted author manuscript

Published in
IUS 2020 - International Ultrasonics Symposium, Proceedings

Ultrasound Imaging of the Brain using Full-Waveform Inversion

1st Ulas Taskin
Department of Imaging Physics
Delft University of Technology
Delft, the Netherlands
u.taskin@tudelft.nl

2nd Kjersti Solberg Eikrem
NORCE Norwegian Research Centre AS
Bergen, Norway
kjei@norceresearch.no

3rd Geir Nævdal
NORCE Norwegian Research Centre AS
Bergen, Norway
gena@norceresearch.no

4th Morten Jakobsen
Department of Earth Science
University of Bergen
Bergen, Norway
Morten.Jakobsen@uib.no

5th Dirk J. Verschuur
Department of Imaging Physics
Delft University of Technology
Delft, the Netherlands
D.J.Verschuur@tudelft.nl

6th Koen W. A. van Dongen
Department of Imaging Physics
Delft University of Technology
Delft, the Netherlands
K.W.A.vanDongen@tudelft.nl

***Abstract*—Transcranial ultrasound has been used to image the brain since 1942. Currently, it is regaining interest and full-waveform inversion (FWI) methods are now employed to reconstruct speed-of-sound profiles of the brain. Many of these methods require a good starting model. Here, we test the applicability of contrast source inversion (CSI) as a FWI method to reconstruct two-dimensional speed-of-sound profiles of the soft brain tissue enclosed by the skull. The advantage of CSI is that it can handle large acoustic contrasts without the need for a good starting model. To test the performance of CSI, we first compute synthetic data. The resulting pressure field clearly shows a significant amount of multiple scattering caused by the skull that acts as a hard acoustic contrast. Next we invert the resulting synthetic data within the Born approximation as well as by applying CSI as a FWI method. The results clearly show that Born inversion can only image the soft brain tissue in the absence of the skull whereas it generates erroneous results when the skull is present. On the other hand, with CSI it is feasible to reconstruct both the skull and the soft brain tissue accurately. Importantly, as compared to other methods CSI does not require any a priori information about the contrast, a mask or a heterogeneous starting model to reconstruct the soft tissue enclosed by the skull.**

***Index Terms*—transcranial ultrasound, brain, full-waveform inversion, quantitative imaging, speed-of-sound profile**

I. Introduction

Transcranial ultrasound (US) as a modality to image the brain is gaining interest as an alternative for expensive MRI scans or radiation based CT scans. Although started in the early forties by Dussik [1], it only revived recently by the application of full-waveform inversion (FWI) methods to image the soft tissue in the brain [2]. FWI methods are commonly used for seismic applications [3]. With transcranial ultrasound, FWI methods are needed to account for the enormous amount of multiple scattering due to the presence of the large acoustic contrasts in the head, i.e. the skull and the various air cavities. In addition to imaging and inversion, FWI methods are needed to model the acoustic wavefield when transcranial ultrasound is used for tumor ablation [4], [5].

The FWI methods used in the past by Guasch et al. either need a good starting model (e.g. obtained from a CT scan) or the application of an Adaptive Waveform Inversion (AWI) method. With AWI, a starting model from the data is constructed and successively used as input for their conventional FWI method [2]. Here we test the applicability of Contrast Source Inversion (CSI) as a FWI method to reconstruct speed-of-sound profiles of the brain and the skull [7], [8]. CSI is known to work well in the absence of a good starting model, the previously presented switch, or any additional regularization [6]. To test our FWI method, we first solve the forward problem using a conjugate gradient method [9], [10]. To investigate the effect of the skull on the resulting pressure field we model the wave field in the presence and the absence of the skull. Due to the low frequencies employed, we can neglect attenuation [10]. Finally, we process our synthetically recorded wavefields using three different imaging/inversion methods: SAFT, Born inversion (BI) and CSI [8].

II. Theory

The two-dimensional acoustic problem of interest is formulated in the temporal Fourier domain with angular frequency ω using the following integral equation formulation

$$p(\mathbf{x}) = p^{\mathrm{inc}}(\mathbf{x}) + \omega^2 \int_{\mathbb{D}} G(|\mathbf{x}-\mathbf{x}'|)\chi(\mathbf{x}')p(\mathbf{x}')\mathrm{dA}(\mathbf{x}'), \quad (1)$$

where $p(\mathbf{x})$ and $p^{\mathrm{inc}}(\mathbf{x})$ are the total and incident pressure fields at the location $\mathbf{x}$ respectively, $G(|\mathbf{x}-\mathbf{x}'|)$ is the Greens function, and where

$$\chi(\mathbf{x}') = \frac{1}{c^2(\mathbf{x}')} - \frac{1}{c_0^2}, \quad (2)$$

is the contrast function with $c(\mathbf{x}')$ and c_0 being the speed of sound of the contrast and the embedding respectively. Note that the contrast is only non-zero in the spatial domain $\mathbb{D}$, where $\mathbb{D}$ is enclosed by the domain $\mathbb{S}$ that contains the sources

and the receivers. To compute synthetic measurement data, integral equation (1) is solved using a conjugate gradient scheme. To reduce computing time, without losing accuracy, a reduced implementation of the forward operator is employed [9], [10].

For imaging and inversion we use three methods: SAFT, BI and CSI [8]. With BI, integral equation (1) is linearized by replacing the unknown total pressure field inside the integral equation with the known incident pressure field $p^{\mathrm{inc}}(\mathbf{x})$. Hence, for BI the employed integral equation reads

$$p(\mathbf{x}) = p^{\mathrm{inc}}(\mathbf{x}) + \omega^2 \int_{\mathbb{D}} G(|\mathbf{x}-\mathbf{x}'|)\chi(\mathbf{x}')p^{\mathrm{inc}}(\mathbf{x}')\mathrm{dA}(\mathbf{x}'). \quad (3)$$

However, as results will show, the skull will give rise to a significant amount of multiple scattering that can't be neglected. As a result of this, it is necessary to employ a full-waveform inversion method. In this work, we use CSI. To this end we formulate integral equation (1) as

$$p^{\mathrm{sct}}(\mathbf{x}) = \omega^2 \int_{\mathbb{D}} G(|\mathbf{x}-\mathbf{x}'|)w(\mathbf{x}')\mathrm{dA}(\mathbf{x}'), \quad (4)$$

where the contrast source $w(\mathbf{x}')$ is defined as

$$w(\mathbf{x}') = \chi(\mathbf{x}')p(\mathbf{x}'). \quad (5)$$

With CSI, the unknown contrast source is updated using an iterative scheme that minimizes the following cost function E

$$E = \eta_{\mathbb{S}}\|p^{\mathrm{sct}} - \mathrm{L}^{\mathbb{S}}[w]\|^2_{\mathbb{S}} + \eta_{\mathbb{D}}\|\chi p^{\mathrm{inc}} - w + \chi\mathrm{L}^{\mathbb{D}}[w]\|^2_{\mathbb{D}}, \quad (6)$$

where $\eta_{\mathbb{S}}$ and $\eta_{\mathbb{D}}$ are normalization terms, and where $\mathrm{L}^{\mathbb{D}}$ and $\mathrm{L}^{\mathbb{S}}$ are integral operators derived from equation (4). After each update of the contrast source $w(\mathbf{x})$, both the pressure field $p(\mathbf{x})$ inside $\mathbb{D}$ as well as the $\chi(\mathbf{x})$ (and hence $c(\mathbf{x})$) are updated.

III. Results

To test the presented imaging and inversion methods for transcranial ultrasound we compute synthetic measurement data for the two head models shown in figure 1. The two-dimensional models are derived from a MRI scan and only show variations in the speed of sound [11]. The differences between the two models is the absence or the presence of the skull; with the first model the skull is replaced by water whereas with the second model the skull is left intact. This adaption of the model is done to investigate the effect of the skull on the resulting pressure field as well on the imaging and inversion results.

Less sources ($N_{src} = 32$) than receivers ($N_{rec} = 256$) are used to scan the model. It has been shown previously that this will lead to a significant reduction in computational load and inversion time - without hardly any loss in convergence rate - when FWI is employed [12].

The employed source wavelet for the probing wave field is shown in figure 2; a Gaussian modulated pulse with a center frequency $f_0 = 0.1$ MHz. Although the bandwidth of the signal is representative for medical ultrasound, its center frequency is relatively low. This is done to avoid cycle skipping as well as to be able to handle the large acoustic

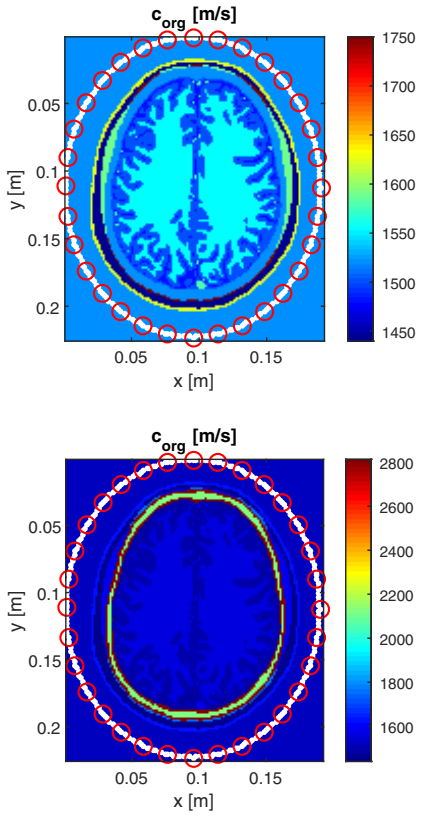

Fig. 1. Speed-of-sound profile in the absence (top) and the presence (bottom) of a skull. The two-dimensional model is surrounded by 32 sources (red circles) and 256 receivers (white dots).

contrast during the inversion. The 110 frequency components used for the inversion are indicated by the red dots. Due to the low center frequency of the employed source wavelet, attenuation by absorption can be neglected [10]. To reduce the computing time required to solve the forward problem, we use a reduced forward operator formulation without any loss on accuracy [9]. Finally, space and time are discretised using step sizes of $\Delta x = 1.5$ mm and $\Delta t = 2.5$ μs respectively.

To test the effect of the skull on the resulting wave field, the forward problem is solved twice: first in the absence of skull (the skull is replaced by water) and second in the presence of the skull. Snapshots of the resulting wave field for both cases at $t = (60.0, 122.5, 185.0, 247.5, 310.0, 372.5, 435.0)$ μs are shown in figure 3. These results clearly show that the skull has an enormous effect on the pressure field. The snapshots clearly show that a vast amount of multiple scattering is generated by the skull; i.e. in the absence of the skull there is hardly any wave field visible after 310 μs, whereas in the presence of a skull the scattered field remains clearly visible in all remaining snapshots. Although not clearly visible in the presented results, animations of the computed wave fields show that the skull act as a kind of "wave guide" for the acoustic field.

The resulting profiles obtained with imaging (SAFT) and inversion (BI and CSI) are shown in figure 4. Due to the low frequencies employed, SAFT fails for both cases. BI does

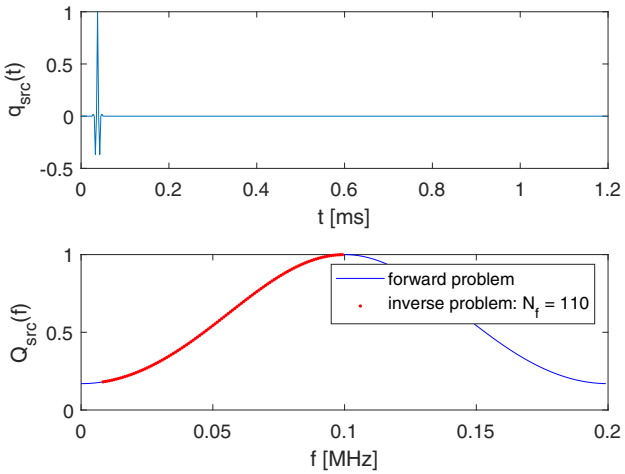

Fig. 2. Source wavelet in time (left) and frequency (right) domain. The red dots indicate the frequency components used for inversion.

succeed in making an accurate reconstruction of the soft tissue in the absence of the skull but not in its presence. In the latter case, BI is capable of imaging the skull itself but it fails to reconstruct the soft tissue enclosed by the skull. In addition, all multiple scattering present in the data for the second case is projected at the location of the receivers as this type of scattering is not taken into account with the employed formalism. Only CSI succeeds in reconstructing the head model and in particular the soft brain tissue; both in the absence and in the presence of the skull. The results clearly show that with CSI an accurate speed-of-sound profile can be reconstructed with correct values for the various soft tissues enclosed by the skull.

IV. Conclusion

The presence of a vast amount of multiple scattering - caused by the skull and clearly visible in the data - prohibits the applicability of SAFT or Born inversion based methods for transcranial ultrasound. Here we show that Contrast Source Inversion as a full-waveform-inversion (FWI) method can be successfully used to process synthetic transcranial ultrasound data. The resulting image shows an accurate reconstruction of the speed-of-sound profile of the head in which the skull and the structure of the soft brain tissues are clearly visible. Importantly, this excellent reconstruction is obtained without the use of any a priori information; i.e. no mask or heterogeneous starting model has been used during inversion.

References

[1] K. T. Dussik, "On the possibility of using ultrasound waves as a diagnostic aid," Zeitschirft fü r die gesamte Neurologie und Psychiatrie, vol. 174, no. 1, pp. 153–68, 1942.

[2] L. Guasch, O. Calderón Agudo, M. Tang, P. Nachev, and M. Warner, "Full-waveform inversion imaging of the human brain," npj Digital Medicine volume, vol. 3, no. 28, 2020.

[3] J. Virieux, and S. Operto, "An overview of full-waveform inversion in exploration geophysics," Geophysics, vol. 74, no. 6, pp. 1–26, 2009.

[4] G. A. Meles, J. van der Neut, K. W. A. van Dongen, and K. Wapenaar, "Wavefield focusing with reduced cranial invasiveness," 2019 IEEE International Ultrasonics Symposium (IUS), pp. 1851–1854, 2019.

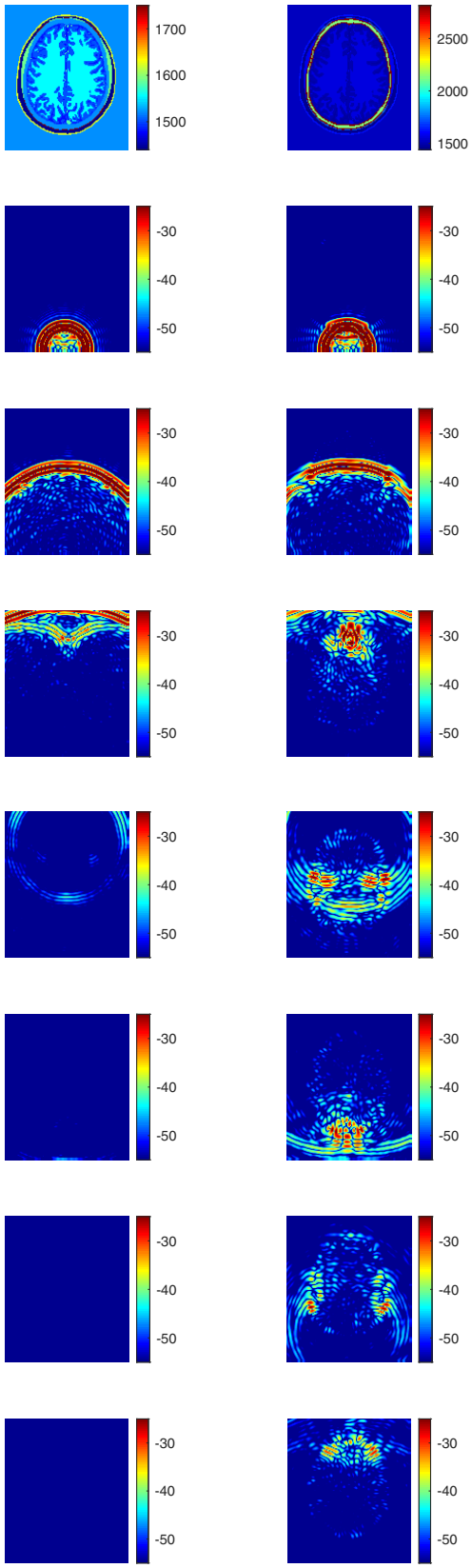

Fig. 3. A full-wave method is used to compute synthetic data in the absence (left) and the presence (right) of the skull. The employed speed of sound profile (top row) and the resulting pressure fields. The snapshots of the wave field are taken at $t = (60.0, 122.5, 185.0, 247.5, 310.0, 372.5, 435.0)$ μs.

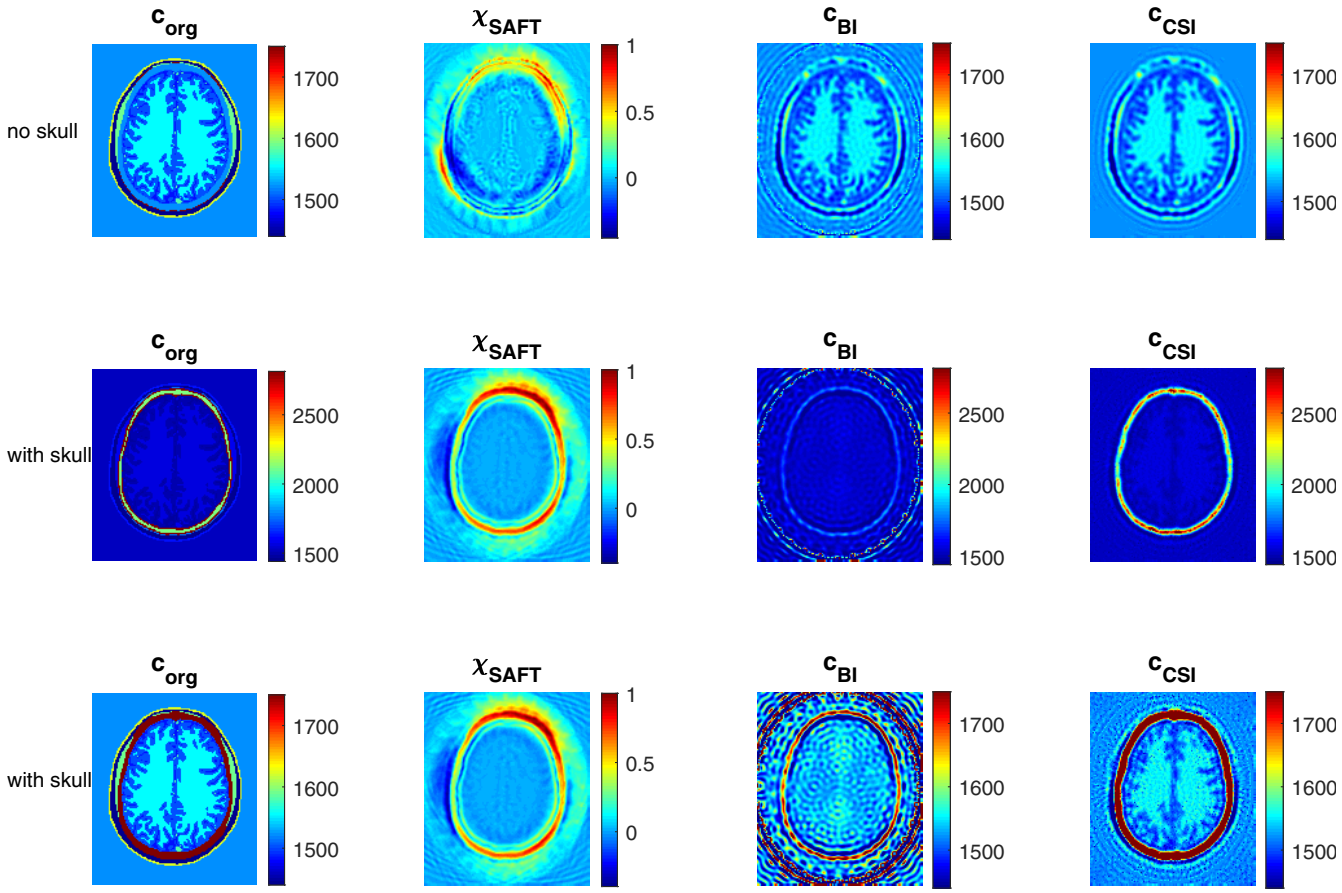

Fig. 4. From left to right: original speed-of-sound profile, SAFT, Born Inversion (BI), and Contrast Source Inversion (CSI). Top row: no skull - Middle row: with skull - Bottom row: same results as shown in the middle row, but now with the amplitudes scaled according to first row.

[5] G. A. Meles, J. van der Neut, K. W. A. van Dongen, and K. Wapenaar, "Wavefield finite time focusing with reduced spatial exposure," The Journal of the Acoustical Society of America, vol. 145, no. 6, pp. 3521–3530, 2019.

[6] A. B. Ramirez and K. W. A. van Dongen, "Sparsity constrained contrast source inversion," The Journal of the Acoustical Society of America, vol. 140, no. 3, pp. 1749–1757, 2016.

[7] P. M. van den Berg, and A. Abubakar, "Contrast source inversion method: State of art," Progress in Electromagnetics Research, vol. 34, pp. 189–218, 2001.

[8] N. Ozmen, R. Dapp, M. Zapf, H. Gemmeke, N. V. Ruiter, and K. W. A. van Dongen, "Comparing different ultrasound imaging methods for breast cancer detection," IEEE Transactions on Ultrasonics, Ferroelectrics, and Frequency Control, vol. 62, no. 4, pp. 637–646, 2015.

[9] K. W. A. van Dongen, C. Brennan, and W. M. D. Wright, "Reduced forward operator for electromagnetic wave scattering problems," IET Science, Measurement & Technology vol. 1, no. 1, pp. 57–62, 2007.

[10] U. Taskin, N. Ozmen, H. Gemmeke, and K. W. A. van Dongen, "Modeling breast ultrasound; on the applicability of commonly made approximations," Archives of Acoustics, vol. 43, no. 8, 2018.

[11] M. I. Iacono, E. Neufeld, E. Akinnagbe, K. Bower, J. Wolf, I. Oikonomidis, D. Sharma, B. Lloyd, B. Wilm, M. Wyss, K. Pruessmann, A. Jakab, N. Makris, E. Cohen, N. Kuster, W. Kainz, and L. M. Angelone, "MIDA: A Multimodal Imaging-Based Detailed Anatomical Model of the Human Head and Neck," in PLoS ONE, vol. 10, no. 4: e0124126. doi:10.1371/journal.pone.0124126, 2015.

[12] A. B. Ramirez and K. W. A. van Dongen, "Can sources and receivers be interchanged for imaging?," 2016 IEEE International Ultrasonics Symposium (IUS), pp. 1–4, 2016.